Open Access Library Journal
2023, Volume 10, e9898
ISSN Online: 2333-9721
ISSN Print: 2333-9705

Fluid Inclusion Characteristics and Hydrocarbon Accumulation Significance of Shanxi Formation in Daning-Jixian Area

Xiao Yang[1,2], Wuernisahan Maimaitimin[1,2], Jiayi Fan[1,2], Zhiwei Du[1,2]

[1]School of Earth Science and Engineering, Xi'an Shiyou University, Xi'an, China
[2]Key Laboratory of Hydrocarbon Accumulation of Shaanxi Province, Xi'an Shiyou University, Xi'an, China
Email: 2602866583@qq.com

How to cite this paper: Yang, X., Maimaitimin, W., Fan, J.Y. and Du, Z.W. (2023) Fluid Inclusion Characteristics and Hydrocarbon Accumulation Significance of Shanxi Formation in Daning-Jixian Area. *Open Access Library Journal*, **10**: e9898.
https://doi.org/10.4236/oalib.1109898

Received: February 21, 2023
Accepted: March 20, 2023
Published: March 23, 2023

Abstract

In order to clarify the gas accumulation process of Upper Paleozoic in Daning-Jixian area, the fluid inclusions in the study area were tested and analyzed comprehensively by single polarizing microscope observation, laser Raman spectroscopy analysis and microthermometry. Finally, the accumulation period was determined based on burial history. The results show that there are five types related to hydrocarbon accumulation in the study area, and the hydrocarbon inclusions mainly include the following four types: 1) methane inclusions; 2) asphalt-containing methane inclusions; 3) asphaltene inclusion; 4) methane inclusions containing CO_2. The inclusions are mainly distributed in the healed microcracks, quartz edge enlarging and cracks, and the hydrocarbon inclusions are mainly distributed in the healed microcracks. Combined with the homogenization temperature of inclusions and the recovery results of thermal evolution history, the first stage was the kerogen cracking gas stage, and the homogenization temperature range of associated brine inclusions was 100˚C - 170˚C, and the main charging time was estimated to be 120 - 205 Ma. In addition, according to the characteristic peaks of a large number of asphaltene inclusions (or asphaltene-containing methane inclusions) in Raman test results, it is speculated that there is a second accumulation stage, namely the cracking stage of wet gas and condensate oil. Combined with the measured organic matter Ro > 2.0% in the study area, the corresponding time of the pyrolysis charging period was determined to be 100 - 120 Ma when projected into the thermal evolution history.

Subject Areas

Petroleum Geology

Keywords

Fluid Inclusion, Accumulation Period, Accumulation Process, Shanxi Formation, Ordos Basin

1. Introduction

In the process of mineral crystallization and growth, the part of a material that is wrapped in mineral lattice defects or holes, and is still sealed up in the main mineral, and has a phase boundary with the main mineral is called fluid inclusion [1]. As one of the most direct and effective methods to study fluid properties in a paleodiagenetic environment, fluid inclusions contain abundant information about paleo-temperature, pressure and paleo-fluid composition. Therefore, geologists have gradually applied it to the study of petroleum exploration and the hydrocarbon accumulation period, which has become an important link in oil and gas exploration and has important practical significance to solving the theoretical and practical problems.

The natural gas accumulation law of Upper Paleozoic in Ordos Basin has been studied deeply by the fluid inclusion method. However, there are still different views on the accumulation periods of the Upper Paleozoic in Ordos Basin, and detailed pieces of evidence have been obtained from the first stage [2] [3], the second stage [4] [5] [6], the third stage [7] [8] and the multi-stage [9]. The author believes that the predecessors' views on the accumulation period of the Upper Paleozoic in Ordos Basin are reasonable, and the main reason for the differences is that the specific block has its uniqueness, and the accumulation process is different under the comprehensive influence of various geological factors.

This study attempts to use a variety of analysis and testing methods to summarize the characteristics of fluid inclusions in the study area. Combined with the burial history and thermal evolution history of a single well, the gas accumulation time and accumulation period of Shanxi Formation in Daning-Jixian area are analyzed.

2. Geological Setting

Daning-jixian block of Daji Gas Field in the southeast of Ordos Basin is located in the west of Shanxi Province, spanning Daning, Ji and Pu counties, and tectonically located at the southern end of Jinxi flexural fold belt of Ordos Basin and the southeastern margin of Yishan slope (**Figure 1**). The Ordovician Majiagou Formation, Upper Carboniferous Benxi Formation, Lower Permian Taiyuan and Shanxi Formations, Middle Permian Lower Shihezi and Upper Shihezi Formations, and Upper Permian Shiqianfeng Formation were developed from bottom to top in the Upper Paleozoic [10] [11]. The Permian Shan-23 member is the main production layer, and the 5# coal developed at the top of Shan-23 is one of the main source rocks of the gas field. Its distribution stability is good,

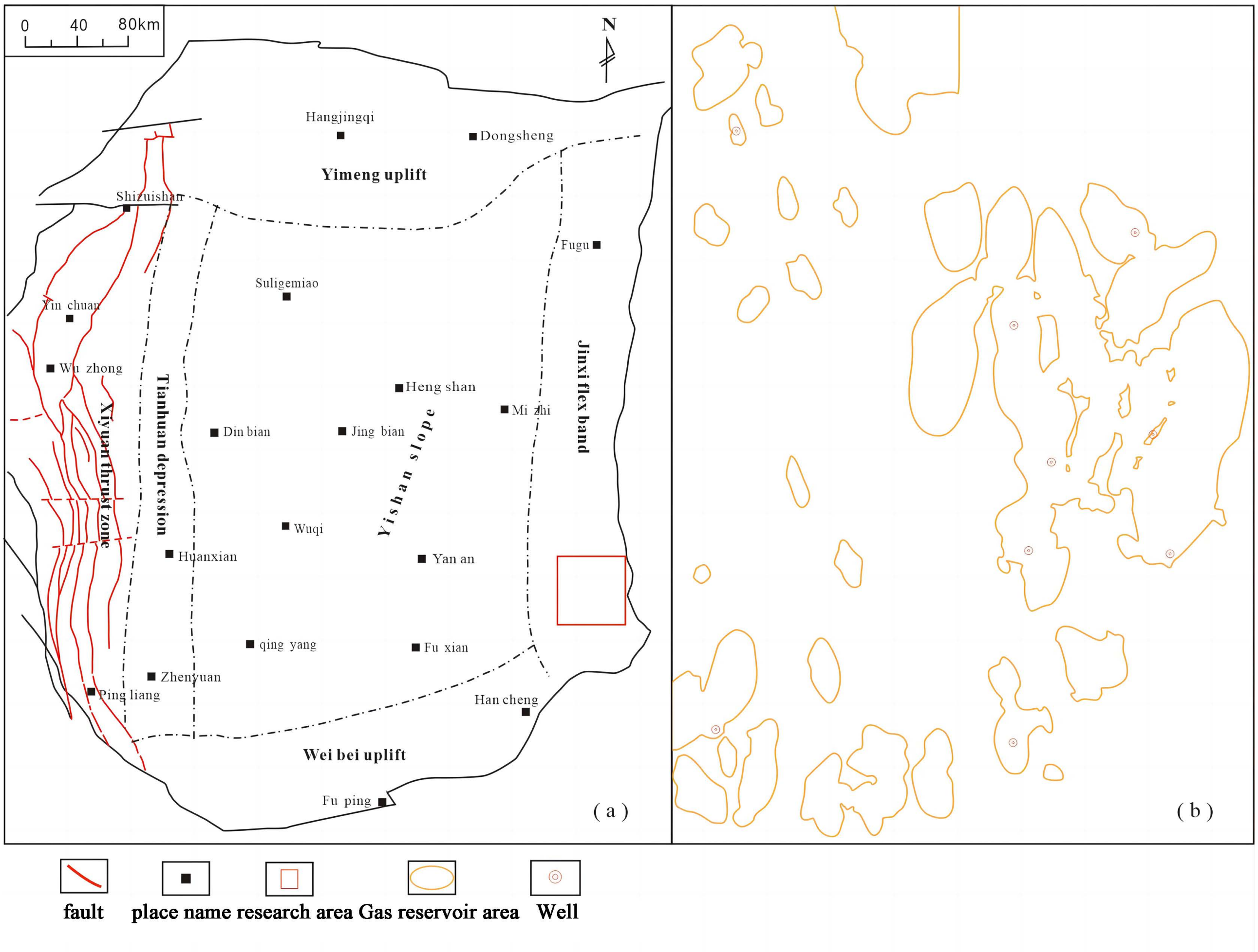

Figure 1. Structural location and sampling well location map of the study area.

and its thickness varies between 1.7 and 7.2 m, showing a ring belt thickening from east and west to the middle [12]. The abundance of organic matter is high, and kerogen types are mainly Ⅱ and Ⅲ, with strong hydrocarbon generation capacity and long duration.

Shan-2 member is mainly a delta coal-bearing stratum, and Shan-1 member is mainly a fluvial delta environment of sand and mudstone deposits. The gas reservoir is mainly composed of lithic sandstone and lithic quartz sandstone. The gas reservoir of Shanxi Formation has poor physical property and strong heterogeneity, with a wide range of porosity and low permeability. The porosity of sandstone of Shan2 Member is 1% - 13%, mainly concentrated in 5% - 7%, and the permeability is basically lower than $0.5 \times 10^{-3}\ \mu m^2$, and the porosity of Shan1 sandstone is 2% - 13%. It is mainly concentrated in 2% - 3%, and the permeability is similar to that of Shan 2, which has typical characteristics of low permeability and tight sandstone gas reservoir. In addition, the difference between this area reservoir and conventional natural gas reservoir lies in the typical "source-reservoir integration" feature of coalbed methane, that is, 5# coal is both source rock and reservoir. Previous studies have shown that 5# coal has a porosity of 1.91% -

4.10%, an average porosity of 2.70%, and a permeability of (0.001 - 11.9) × 10^{-3} μm^2. The regional cap bed is the Lower Shihezi Formation of Permian system, with mudstone of varying thickness and part of argillaceous siltstone, compact lithology and poor permeability, playing a good capping role [13] [14] [15].

3. Sample Collection and Experimental Methods

In this study, fluid inclusion samples and gas-bearing samples were collected from Shanxi Formation (**Table 1**). The petrographic observation was made by Leica 4 M microscope. Renshaw inVia microscope laser Raman spectrometer was used for spectral analysis. Linkam THMS 600 G type cold and hot platform for the determination of homogenization temperature and freezing point temperature, In order to accurately record the time of inclusion homogenization, the measurement error is 0.6˚C, the initial heating rate is 5˚C/min, and the adjustment is 2˚C/min when approaching the homogenization state. The test analysis was completed in Shaanxi Provincial Key Laboratory of Petroleum Accumulation Geology.

4. Fluid Inclusion Characteristics

4.1. Types of Fluid Inclusions

In this study, the intact inclusions in the samples were selected, and the composition of the inclusions was determined by laser Raman spectroscopy. The results showed that the main inclusions of Shanxi Formation in the study area were brine inclusions, and the components of hydrocarbon inclusions were mainly

Table 1. Fluid inclusion sampling of Shanxi Formation in Daning-Jixian area.

Well name	Depth	Layer	Host mineral	occurrence	Log interpretation
D10	1928.2	$Shan_1$	quartz	Extended edge, Healing microfissure	Differential gas layer
D10	1930.5	$Shan_1$	quartz	Healing microfissure	gas layer
D10	1934.2	$Shan_1$	quartz	Healing microfissure	gas layer
D30	1937.35	$Shan_1$	quartz	Extended edge, Healing microfissure	Differential gas layer
D20	1937.6	$Shan_1$	quartz	Extended edge, Healing microfissure	gas layer
D19	2080.15	$Shan_1$	quartz	Healing microfissure	gas layer
G5	2238.35	$Shan_1$	quartz	Healing microfissure	gas layer
H15	2278.8	$Shan_1$	quartz	Healing microfissure	gas layer
D30	2127.8	$Shan_2$	quartz	Healing microfissure	gas layer
D30	2130.9	$Shan_2$	quartz	Healing microfissure	Air and water in the same layer
D2	1919.4	$Shan_2$	quartz	Healing microfissure	gas layer
D53	1912.8	$Shan_2$	quartz	Extended edge, Healing microfissure	Differential gas layer
G5	2263.96	$Shan_2$	quartz	Healing microfissure	gas layer
D19	2151.4	$Shan_2$	quartz	Extended edge	Differential gas layer

CH_4 and asphaltene, and the types included: There are four types of CH_4 inclusion, asphaltene CH_4 inclusion, asphaltene inclusion, and CO_2-methane inclusion (**Figure 2**).

1) Brine inclusion: This kind of inclusion is the most widely distributed, and the volume of many inclusions varies widely. Under the transmitted light, they are colorless and transparent, with "bubbles". 2) CH_4 inclusion: There is only an obvious characteristic peak of methane in the Raman spectrum, and the Raman shift mainly ranges from 2910 to 2914 cm^{-1}. This type of inclusions are mainly gaseous hydrocarbon inclusions, which are dark gray to black under transmitted light [16], and mainly occur in the healed micro-cracks of quartz particles. 3) Bituminous methane inclusions: The Raman spectra not only showed obvious bitumen double peaks, but also detected CH_4 characteristic peaks. The "D" peak

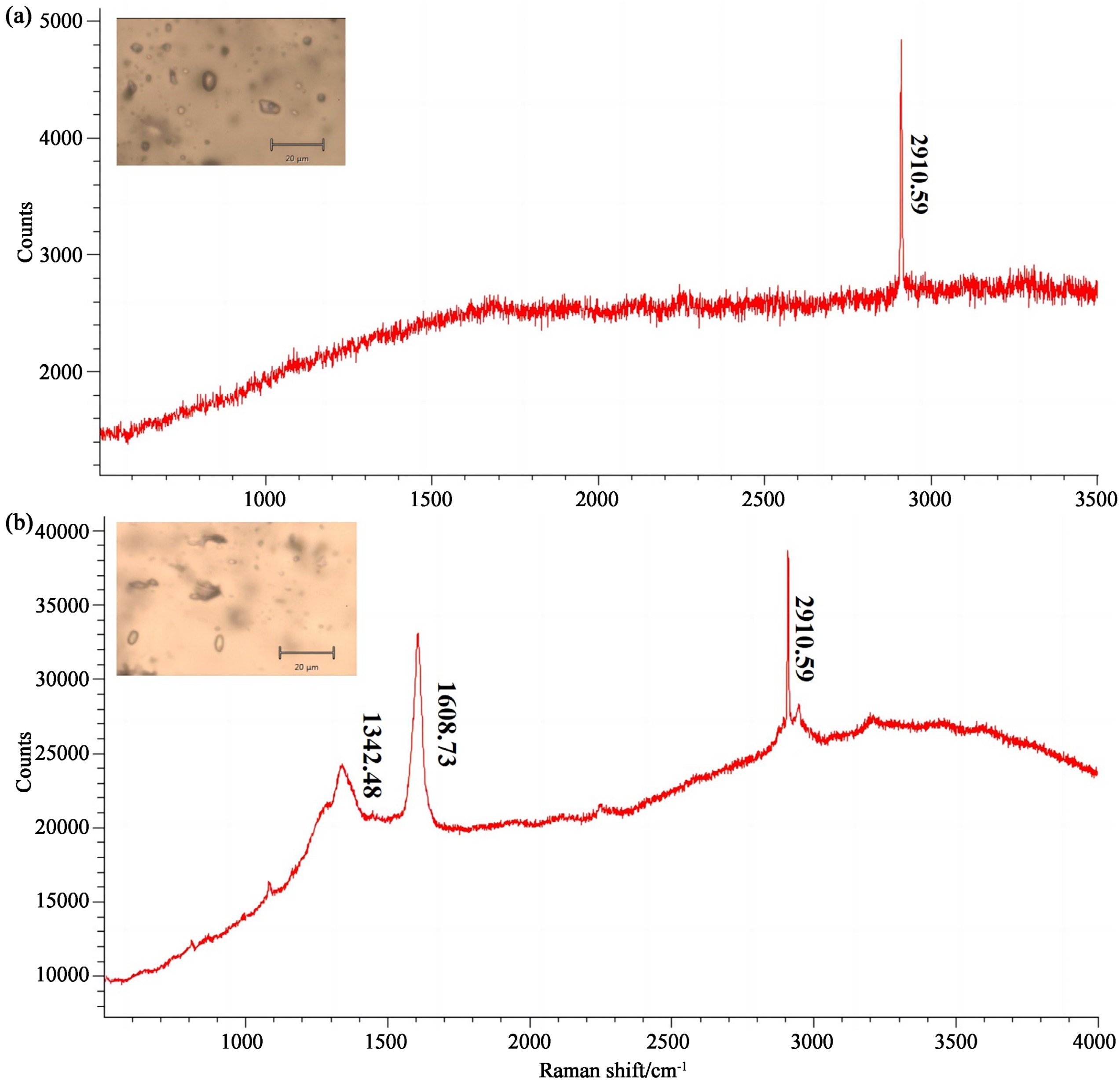

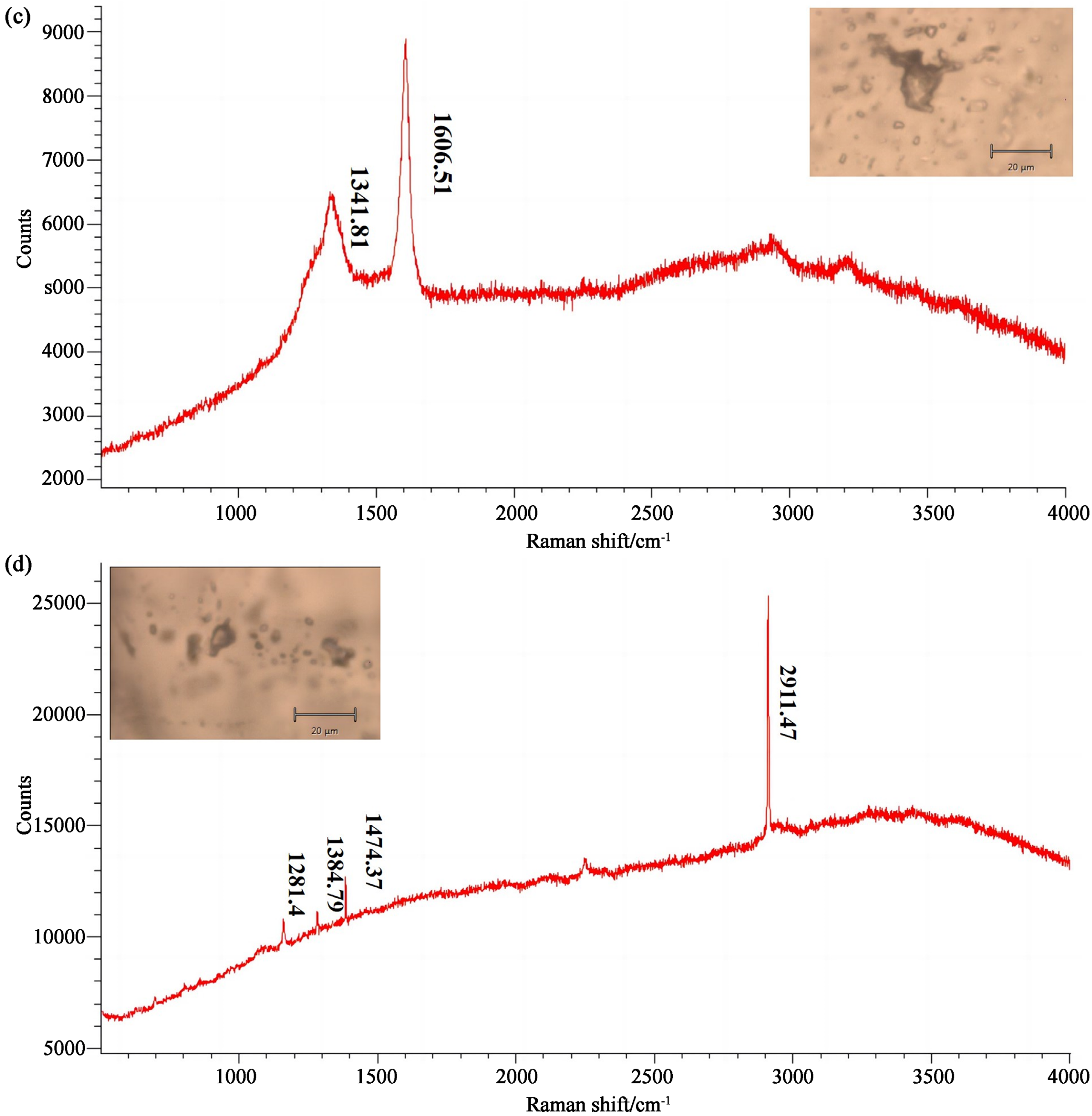

Figure 2. Main types and components of hydrocarbon inclusions from Shanxi Formation in Daning-Jixian area. (a) CH_4 inclusion; (b) Bituminous methane inclusions; (c) Asphaltene inclusion; (d) CO_2-containing methane inclusion.

mainly ranged from 1311 to 1370 cm^{-1}, the "G" peak mainly ranged from 1601 to 1610 cm^{-1}, and the Raman shift peak of methane mainly ranged from 2910 to 2913 cm^{-1} [17] [18]. These kinds of inclusions, which are generally transparent but have black edges, mainly occur in the healed micro-cracks of quartz particles. 4) Asphaltene inclusion: The Raman spectra showed only two peaks of asphalt, 1311 - 1340 cm^{-1} and 1604 - 1608 cm^{-1}, respectively. These inclusions were irregular in shape, black in transmitted light, and mainly distributed along cracks. 5). CO_2-containing methane inclusion: The CO_2-containing methane inclusions are less distributed in the microcracks of quartz grains in a banded manner. Compared with other hydrocarbon inclusions, the color is between bituminous methane inclusions and asphaltene inclusions, and the color is dark and translucent. Raman spectra not only show the typical Fermi resonance twin peaks of CO_2 (1281.4 cm^{-1} and 1384.785 cm^{-1}) [19], but also the obvious characteristic peak of CH_4 (2912.521 cm^{-1}).

4.2. Petrographic Characteristics of Inclusions

Fluid inclusions in Shanxi Formation reservoir in Daning-Jixian area are widely developed, with different sizes, with an average diameter of 1 - 16 μm, and are mainly elliptic, long strip, angular and irregular. The host mineral of the inclusions is mainly quartz, which occurs mostly along the healed microcracks, then in the enlarged edges, and very few in the microcracks. The distribution forms of inclusions are mainly banded, beaded and contiguous, while some inclusions are sporadically distributed (**Figure 3**).

According to the microscopic observation, the characteristics of hydrocarbon inclusions and their associated brine inclusions were summarized, and the occurrence relationship of fluid inclusions in quartz particles was determined. It was found that: 1) The volume of hydrocarbon inclusions was larger than that of the associated brine inclusions in the same occurrence, and the color was darker under transmitted light, mostly dark brown to black, or the overall transparent edge was dark; 2) Generally, for the same quartz particles, there are interleaved micro-cracks distributed in different directions. 3) The phenomenon that the healed microfissure cuts through the enlarged edge or penetrates through the adjacent quartz particles can be observed in some samples, indicating that the formation time of inclusions in the healed microfissure is later than that of the enlarged edge. Most of the cracks are cut through quartz particles, and the formation time is later than the healing of microcracks and the enlargement of edges. The above results show that the inclusions in quartz with enlarged edges are the earliest, and the inclusions distributed in cracks are later than those in healed micro-cracks. However, microscopic observation can only preliminarily classify the relative phases of hydrocarbon inclusions, which requires further comprehensive study combined with Raman test and microthermometry.

4.3. Fluid Inclusion Temperature Measurement

4.3.1. Homogenization Temperature

A total of 166 associated saline inclusions were tested in this experiment, which were mainly distributed in the healed micro-cracks of quartz particles, and a few were distributed in the secondary enlarged edges of quartz. The test results show that the temperature characteristics of Shan1 member and Shan 2 member are similar: the homogenization temperature of the associated brine inclusions in Shanshan 1 member is 79.2˚C - 179˚C, and the main peak temperature is 100˚C - 150˚C. The homogenization temperature of the associated saline inclusions in the second member of the mountain ranges from 83.4 ˚C to 170˚C, and the main

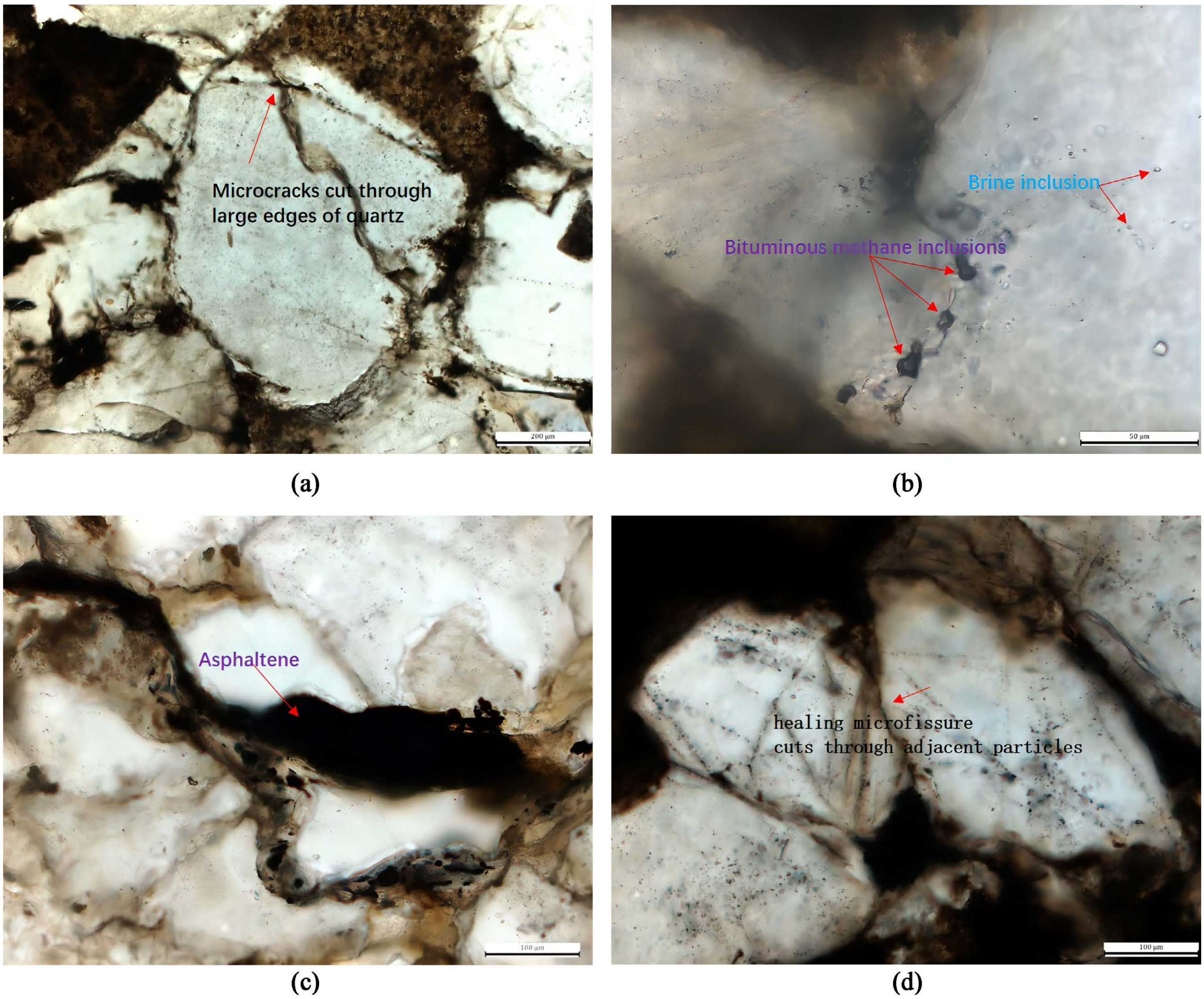

Figure 3. Petrographic characteristics of fluid inclusions of Shanxi Formation in Daning-Jixian area. (a) Microcracks cut through large edges of quartz ((100×), D10, 1937.35 m, $Shan_1$); (b) Bituminous methane inclusions distributed beaded in microfractures ((500×) G5, 2263.96 m, $Shan_2$); (c) Asphaltene distributed in fractures ((200×) D10, 1934.2 m, $Shan_1$); (d) A linear distribution of inclusions along the microfissure cutting through adjacent quartz grains ((200×) D30, 2130.9 m, $Shan_2$).

peak temperature ranges from 100˚C to 160˚C. In terms of the homogenization temperature of inclusions in Shanxi Formation, there was a main accumulation period in the study area, and a small number of high temperature inclusions indicated that there might be a thermal cracking stage.

4.3.2. Salinity

The freezing temperature of fluid inclusions can reflect the salinity and other information of saline solution inside the inclusions. For saline inclusions with low salinity (mass fraction ranging from 0 to 23.3%), the fluid salinity can be determined according to Raoult's law [20]. In this study, empirical formula was used to calculate the salinity of the solution. The results show that the fluid inclusion salinity of Shanxi Formation reservoir in Daning-Jixian block ranges from 0.5 to 17.79% (**Figure 4**), indicating that the fluid inclusion was formed in

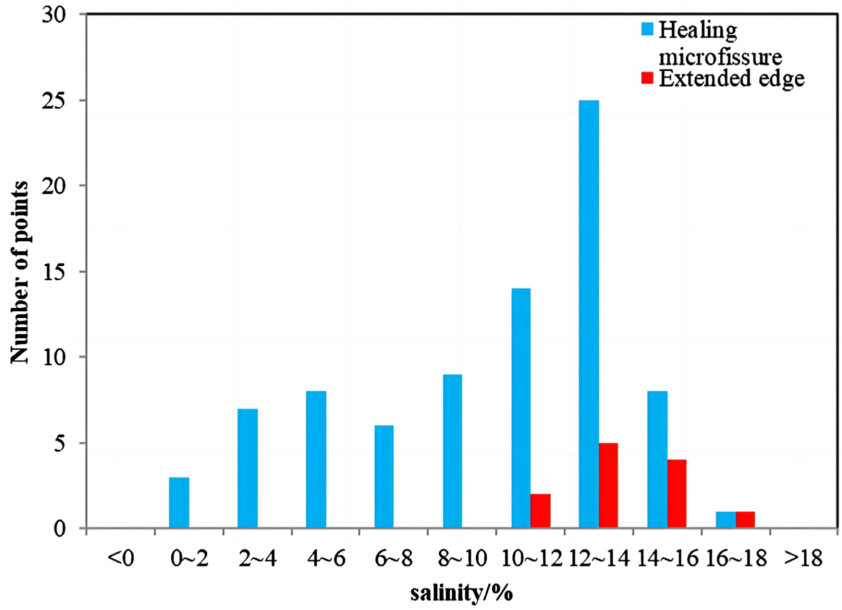

Figure 4. Histogram of salinity distribution in Shanxi Formation.

brackish to brackish water environment. In the intersection diagram of homogenization temperature and salinity, the homogenization temperature distribution is mainly concentrated in the range of 90˚C - 150˚C, and the salinity is mainly in the range of 6% - 15%, which is roughly consistent with the test results of homogenization temperature, and can only show the characteristics of first-stage accumulation.

5. Analysis of Accumulation Stages

The characteristics of fluid inclusions in different diagenetic mineral generations are quite different, which can reflect the degree of hydrocarbon accumulation in the reservoir when these hydrocarbon inclusions are captured to some extent. However, the homogenization temperature of fluid inclusions cannot be used as the basis for determining inclusions and accumulation periods [21]. Therefore, based on detailed observation of petrographic characteristics of different types of inclusions, parameters such as fluid inclusions assemblage, associated brine inclusions homogenization temperature and thermal evolution history within diagenetic mineral generations should be used to comprehensively determine and divide hydrocarbon accumulation periods.

The fluid inclusions of Shanxi Formation in the study area are widely distributed and of various types. The process of gas accumulation in the study area can be effectively analyzed by combining the observation results of lithography, the measurement and calculation of the data of inclusions temperature and salinity, as well as the results of thermal history recovery, so as to provide a scientific basis for further exploration and development.

On the basis of the comprehensive analysis of the inclusion test, combined with the basin's burial history and thermal evolution history, the paleo-geothermal evolution curve of a single well can be restored, and the geological time of oil and gas charging can be roughly estimated, approximately representing the time of oil and gas charging and accumulation. The homogenization temperature of the associated saline inclusions of Shanxi Formation in the study area was projected onto the burial history map of a single well in the area. It can be seen that the gas reservoir of Shanxi Formation in Daning-Jixian area was the first stage of accumulation, which lasted from Jurassic to mid-Early Cretaceous for 100 Ma, during which there was hydrocarbon charging.

6. Conclusions

1) The fluid inclusions in Shanxi Formation reservoir in Daning-Jixian area of Ordos Basin mainly include brine inclusions, methane inclusions, asphaltene inclusions, bituminous methane inclusions and CO_2-containing methane inclusions. The host minerals are mainly quartz, followed by micrite calcite, which are mostly distributed in the healed microcracks, quartz secondary enlarged edges and cracks. The homogenization temperature of the associated saline inclusions in the first member of the mountain ranges from 79.2˚C to 179˚C, and the main peak temperature ranges from 100˚C to 150˚C. The homogenization temperature of the associated saline inclusions in the second member of the mountain ranges from 83.4˚C to 170˚C, and the main peak temperature ranges from 100˚C to 160˚C. The temperature distribution of the inclusions is unimodal, and the peak is narrow in front and wide in back. The temperature distribution characteristics of the inclusions in Shan 1 and Shan 2 are similar.

2) The hydrocarbon generation of coal seams in Shanxi Formation increases formation pressure, which is the main driving force of natural gas accumulation. Asphaltene in fractures indicates that micro-fractures formed under overpressure are the main channel of natural gas migration. With the increase of formation pressure, the adsorption capacity of coal seam increases, and the thick mudstone developed in the first member of Shan Formation provides high-quality cap layer conditions, which makes the formation of the second member of Shan formation maintain a stable high-pressure state, which is conducive to the preservation of coalbed methane.

3) The Upper Paleozoic Shanxi Formation gas reservoir in Daning-Jixian area is a first-stage accumulation, and the charging process is continuous and long, which can be divided into two stages. The first stage was mainly kerogen cracking gas, and the amount and intensity of hydrocarbon charging were small. The homogenization temperature of the associated brine inclusions ranged from 100˚C to 150˚C, corresponding to the Late Jurassic to the middle of Early Cretaceous from 110 to 190 Ma.

Conflicts of Interest

The authors declare no conflicts of interest.

References

[1] Lu, H.Z. (2004) Fluid Inclusion. Science Press, Beijing, 1-487.

[2] Han, Z.H., Zhao, J.Z., Chen, M.N., *et al.* (2020) Reservoir Fluid Inclusion Characteristics and Accumulation Periods of Hehe 8 Member in Western Sulige Gas Field. *Journal of Xi'an Shiyou University* (*Natural Science Edition*), **35**, 18-27.

[3] Li, X.Q., Feng, S.B., Li, J., *et al.* (2012) Geochemistry of Natural Gas Accumulation in Sulige Gasfield, Ordos Basin. *Acta Petrologica Sinica*, **28**, 836-846.

[4] Cao, Q., Zhao, J.Z. and Liu, Y.Q. (2013) Fluid Inclusion Characteristics and Significance of Upper Paleozoic in Southeastern Ordos Basin. *Journal of Northwest University* (*Natural Science Edition*), **43**, 749-756.

[5] Zhao, G.P. (2017) Fluid Inclusion Characteristics and Gas Accumulation Period of Upper Paleozoic Reservoirs in Hangjinqi Area, Ordos Basin. *Oil & Gas Geology*, **38**, 905-912.

[6] Xue, H., Wang, Y., *et al.* (2009) Gas Accumulation Periods of Upper Paleozoic in Northern Ordos Basin: A Case Study of Hangjinqi Exploration Area. *Natural Gas Industry*, **29**, 9-12+136.

[7] Wang, Z.L., Wei, L., Wang, X.Z., *et al.* (2016) Gas Accumulation Process and Mechanism of Lower Paleozoic in Yan'an Area, Ordos Basin. *Acta Petrolei Sinica*, **37**, 99-110.

[8] Ding, C., Chen, G., Guo, L., *et al.* (2011) Hydrocarbon Accumulation Periods of Upper Paleozoic in Northeastern Ordos Basin. *Geological Science and Technology Information*, **30**, 69-73.

[9] Liu, J.Z., Chen, H.H., Li, J., *et al.* (2008) Paleo-fluid Pressure Distribution and Evolution of the 2nd Member of Shanxi Formation Inclusion in Yi-Sban Slope, Ordos Basin. *Acta Petrolei Sinica*, No. 2, 226-230+234.

[10] Li, J., Zhao, J.Z., Wei, X.S., *et al.* (2022) Natural Gas Expansion and Its Accumulation Effect Caused by Stratum Uplift: A Case Study of Sulige Gas Field, Ordos Basin. *Petroleum Exploration and Development*, **49**, 1094-1106.

[11] Li, W.H., Zhang, Q., Li, K.Y., *et al.* (2021) Late Paleozoic Sedimentary Evolution of Ordos Basin and Its Surrounding Areas. *Journal of Palaeogeography*, **23**, 39-52.

[12] Li, W.Z., Chen, G., Sun, B., *et al.* (2011) Reservoir-Forming Conditions and Enrichment Rules of Coalbed Methane in Daning-Jixian Area. *Natural Gas Geoscience*, **22**, 352-360.

[13] Dong, L., Lin, Y.X., Wu, Y.C., *et al.* (2018) Physical Properties and Gas Bearing Characteristics of Main Sandbody Reservoirs in the Upper Paleozoic in Daning-Jixian. *Energy and Environmental Protection*, **40**, 87-94.

[14] Zhao, L.M. Wen, G.H., Li, X.T., *et al.* (2018) Evaluation of Tight Sandstone Gas Reservoir "Sweet Spot" in Daning-Jixian Block, Ordos Basin. *Natural Gas Industry*, **38**, 5-10.

[15] Chen, G. and Li, W.Z. (2011) Influencing Factors and Laws of Deep Coalbed Methane Adsorption Capacity in the Ordos Basin. *Natural Gas Industry*, **31**, 47-49+118.

[16] Liu, D.H., Xiao, X.M., Tian, H., *et al.* (2009) Application of Fluid Inclusion and Bitumen Characteristics to Identify the Origin of Natural Gas. *Petroleum Exploration and Development*, **36**, 375-382.

[17] Zhang, N., Tian, Z.J., Leng, Y.Y., *et al.* (2007) Raman Characteristics of Hydrocarbon and Hydrocarbon Inclusions. *Science in China* (*Series D: Earth Sciences*), No. 7, 900-907.

[18] Liu, D.H., Xiao, X.M., Tian, H., *et al*. (2013) The Types of High Density Methane Inclusions Found in the Northeast Sichuan Basin and the Exploration and Evaluation of Oil Cracking Gas and Shale Gas. *Earth Science Frontiers*, **20**, 64-71.

[19] Chen, Y. and Ernst, A.J. (2009) Principle, Method, Existing Problems and Future Research Direction of Laser Raman Spectroscopy Analysis of Fluid Inclusion. *Geological Review*, **55**, 851-861.

[20] Liu, D.H. (2007) Oil and Gas Inclusions and Their Application in Petroleum Exploration and Development. Guangdong Science and Technology Press, Guangzhou, 1-267.

[21] Tao, S.Z. (2006) The Sequence of Authigenic Minerals Is the Fundamental Basis for Determining the Inclusions Period. *Petroleum Exploration and Development*, No. 2, 154-160.